Available online at www.sciencedirect.com
SCIENCE DIRECT®
Journal of Non-Crystalline Solids 319 (2003) 192–199
JOURNAL OF NON-CRYSTALLINE SOLIDS
www.elsevier.com/locate/jnoncrysol

A Fourier-transform photoluminescence study of radiative recombination mechanism in chalcogenide glasses

N. Asha Bhat [1], K.S. Sangunni *, K.S.R.K. Rao

Department of Physics, Indian Institute of Science, Bangalore 560 012, India

Received 25 January 2002; received in revised form 30 August 2002

Abstract

In this paper, we report photoluminescence (PL) studies carried out using Fourier-transform method in glassy Se (a-Se) and Ge-based $Ge_{20}Se_{80}$ and $Ge_{20}Se_{70}Te_{10}$ glasses. It was observed that the PL spectra of a-Se as well as that of Ge-based glasses exhibit fine features. The details of these fine features are extracted by deconvoluting the experimental spectra and are explained based on phenomenological defect models. Utilizing the deconvoluted information, the radiative recombination transitions occurring at 'valence-alternation pairs' are distinguished from those occurring at 'intimate valence-alternation pairs' and are illustrated with the help of a configurational coordinate diagram representation.

PACS: 71.55.Jv; 78.55.Hx; 78.60.−b; 81.05.Gc

1. Introduction

The presence of inherent defects profoundly influences many light-induced and electronic properties of amorphous/glassy chalcogenides [1,2]. At present, the defects in chalcogenide glasses are understood mainly based on the two phenomenological models namely charged dangling bonds (CDB) model and valence-alternation pair (VAP) model [3–5]. According to the CDB model, the inherent defects, denoted as D^+–D^- charged pairs, are formed due to the rearrangements of unpaired spins at the nearby ends of two chalcogen chains. The same defects in VAP model are denoted as over-coordinated C_3^+ and under-coordinated C_1^- VAPs, respectively, where the superscript denotes the charge and subscript denotes the coordination number. In VAP model, the C_3^+–C_1^- VAPs formed close to each other due to the Coulomb attraction are termed as intimate valence-alternation pairs (IVAP). Alternatively, the VAP and the IVAP C_3^+–C_1^- defects are also termed as random and non-random D^+–D^- defects, respectively, [5].

The under- and -over-coordinated intrinsic defects discussed above are considered to be the major contributors to the gap-states in chalcogenide glasses. Photoluminescence (PL) is one of the

* Corresponding author. Tel.: +91-80 394 2720; fax: +91-80 360 2602.
E-mail address: sangu@physics.iisc.ernet.in (K.S. Sangunni).
[1] Present address: GE India Technology Center, Bangalore 560 066, India.

0022-3093/03/$ - see front matter
doi:10.1016/S0022-3093(02)01918-X

effective characterization techniques that can provide simultaneous information on both shallow and deep level defects and gap-states in many semiconductors [6]. The technique was used extensively in 1970s for studying defects and gap-states in chalcogenide glasses too [7]. The notable findings of these studies were the broad featureless spectra for majority of chalcogenide glasses peaking at nearly half the band gap energies. Exceptions to the featureless spectra were the cases of a few Ge-based amorphous/glassy chalcogenides that exhibited features in the broad spectra, the most recent case being the PL spectra observed in Ge–Se–Bi amorphous films [7,8]. Based on the earlier studies and the trends from PL excitation spectra, the contribution to luminescence in chalcogenide glasses has been considered to be due to the D^+ and/or D^- charged defects [5]. However, the existing identification of PL transitions with random and non-random D^+–D^- defects (or VAP and IVAP centers) has not been unequivocal as the information available in the broad PL spectra of many chalcogenide glasses is not sufficient enough in distinguishing the involvement of VAPs and IVAPs in PL transitions [2,5]. As a result, the *precise details* of luminescence processes in chalcogenide glasses are still to be understood [2].

Until recently, the monochromator dispersion or grating spectroscopy has been the general technique to study absorption or luminescence spectroscopy in visible region of light radiation. It is a known fact that grating spectroscopy does not make the most effective use of limited power of light radiation having wavelengths greater than 1000 nm (or $E < 1.24$ eV) [9]. However, spectroscopic studies using Fourier-transform (FT) method make efficient use of the available power of light radiation having energies less than about 1.3 eV with the help of a basic process namely the light wave interference [9]. With the phenomenal advances in desktop computing since 1980s, the FT method is emerging as the preferred method to carry out spectroscopic studies in recent years. Nonetheless, most of the PL studies in chalcogenide glasses were carried out in pre- or early 1980s era and were largely dependent on the monochromator dispersion method [7,10–12]. A few recent PL studies in chalcogenide glasses are also carried out by dispersing the luminescence through a monochromator [13–15]. To the best of our knowledge, the FT method has not been used so far to study systematically luminescence processes in chalcogenide glasses.

In the present study, our aim was to utilize the FT method to investigate and improve the existing knowledge on the luminescence processes and radiative recombination mechanism in chalcogenide glasses. The samples chosen to do so were elemental a-Se and Ge-based $Ge_{20}Se_{80}$ and $Ge_{20}Se_{70}Te_{10}$ glasses. The Ge-based glasses were chosen specially to explore the scope of modern computing facilities to deconvolute any observable features in the PL spectra of Ge-based glasses and to get therewith better insights into the luminescence processes in these glasses.

2. Experimental details

The samples of interest were prepared by conventional rapid quenching of melts at 1000 °C. To prepare the melts, appropriate amount of 5 N pure elemental materials were taken in silica tubes of 8 mm diameter and were subsequently vacuum-sealed. The sealed ampoules were kept in a long ceramic tube and were loaded into a resistance wound tubular furnace. The furnace was maintained at 1000 °C for 24 h to allow the constituent elements to react properly. The ampoules were then rotated with the help of an external motor for another 24 h to achieve homogenization of the melt. Subsequently the melts were quenched in ice-water + NaOH bath. The samples prepared in this way were confirmed to be X-ray amorphous. Differential scanning calorimetry scans were carried out on the samples to determine the glass-transition temperatures.

Samples having surface dimensions of nearly 2×2 mm^2 were selected for PL studies. The samples had shiny surfaces in their as-prepared form and were used without subjecting to further polishing. A FT photoluminescence spectrometer (MIDAC Corp., USA) was used to carry out present investigations. Samples to be examined were mounted on a sample holder that had provision to mount 20 samples at a time and then

were suspended in a liquid helium cryostat attached to the spectrometer. An argon ion (Ar^+) laser ($\lambda = 514.5$ nm, $E = 2.41$ eV) with 2 mm beam diameter was used as an excitation source. The experiment was carried out at 4.2 K with 150 $mW\,cm^{-2}$ excitation power. PL signals coming from the samples were analyzed by a Michelson Interferometer and were detected with the help of a liquid-nitrogen cooled Ge-photodiode. The interferograms spanning the entire 0.6–1.85 eV range and having 2 meV resolution were recorded by averaging out 10 coadded scan in nearly 30 s using a personal computer attached to the spectrometer. The excitation was turned on just before recording each spectrum. Prior to subjecting the samples of interest to PL studies, it was confirmed each time that semiconducting CdTe placed in some other slot of the same sample holder and taken as the reference showed its characteristic PL spectrum with fine features in 1.35–1.5 eV range [16].

3. Results

The PL spectra recorded at 4.2 K for a-Se and Ge-based $Ge_{20}Se_{80}$ and $Ge_{20}Se_{70}Te_{10}$ glasses are shown in Fig. 1. The luminescence spectra of all the three samples fall in a broad energy range 0.7–1.2 eV. On the whole, PL intensity for $Ge_{20}Se_{80}$ and $Ge_{20}Se_{70}Te_{10}$ is significantly higher compared to that for a-Se. In addition, the overall PL lineshape for each of the three samples is characterized by fine features, the first of its kind for a-Se.

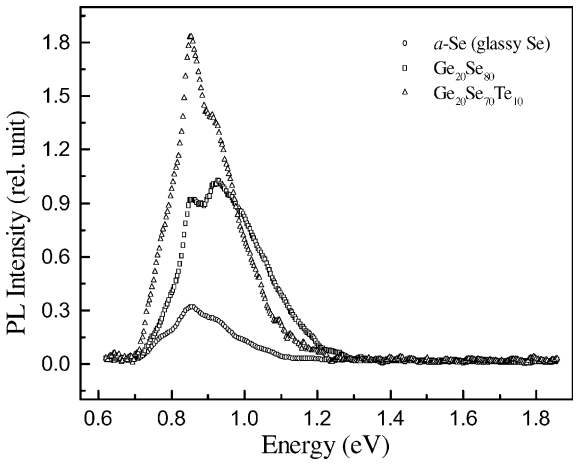

Fig. 1. Experimental PL Spectra for a-Se, $Ge_{20}Se_{80}$ and $Ge_{20}Se_{70}Te_{10}$ glasses recorded at 4.2 K. In each spectrum only alternate data-points (~4 meV step) are shown.

4. Discussion

Firstly, the range of luminescence emission energies appears to be nearly the same irrespective of the composition. In case of melt-quenched glasses containing chalcogen elements, concentration of randomly distributed D^+ and D^- centers or VAPs can be estimated using

$$N_{VAP} = N_0 \exp\left(-\frac{E_{VAP}}{2k_B T_g}\right), \quad (1)$$

where N_0 is the chalcogen atomic density, E_{VAP} is the creation energy for VAP and T_g is the glass-transition temperature [2]. For Se, values of $N_{VAP} \sim 10^{18}$ cm^{-3}, $N_0 \sim 10^{22}$ cm^{-3} and $T_g \sim 320$ K give $E_{VAP} \sim 0.8$ eV, well within the energy range of experimental luminescence spectra [4]. Proceeding along similar lines, when fourfold coordinated Ge atoms that do not have any preferential charged state are added to Se as in $Ge_{20}Se_{80}$, the VAP creation energy remains at around 0.8 eV on account of the increase in glass-transition temperature ($T_g \sim 410$ K) that almost compensates the reduction in N_{VAP}. When Te, again a chalcogen element, replaces 10 at.% of Se as in $Ge_{20}Se_{70}Te_{10}$, the VAP creation energy remains nearly the same again as the chalcogen atomic density and the T_g remain almost unchanged. These observations give an overall indication that the VAP defects are the common centers involved in the PL transitions in all the three samples.

The significantly higher PL intensity of $Ge_{20}Se_{80}$ compared to that of a-Se suggests higher PL efficiency for the former than the latter. The observations are in line with the experimental studies in Ge_xSe_{1-x} glasses wherein a change in x from zero to 1/3 brings out four orders of magnitude increase in PL efficiency [17]. Such an increase is generally attributed to the branching and shortening of Se chains with an increase in the number of unsatisfied bonds and a corresponding increase in D^+–D^- centers [18]. Addition of Te further shortens Se

chains and brings out a marginal increase in PL intensity of $Ge_{20}Se_{70}Te_{10}$ glass as compared to that of $Ge_{20}Se_{80}$ glass. Such an increase is in agreement with the enhanced luminescence efficiency observed when Te is added to Se [19]. In addition, the low luminescence efficiency in a-Se can be attributed to the creation of metastable non-radiative defect centers, confirmation regarding which are available in literature [20].

In Fig. 1, clear fine structure observed for all the spectra including the one for a-Se suggest radiative emission occurring *at least* at three different energies. The observed luminescence line-shapes for Ge-based glasses though more or less conform to the typical shapes observed in the past, the fine features observed for a-Se are first of its kind and were found to be repeatable and reproducible, even for some other samples discussed elsewhere [21]. Absence of such fine features in the past, especially for a-Se having low luminescence efficiency, was probably due to the uncertainties of the order of about 0.04 eV introduced by the monochromator dispersion that could have obscured the finer details of the spectra in majority of the earlier investigations [7]. The possibility looks more likely as it is well known that the FT method followed by us has established advantages over the dispersive grating monochromator technique, especially in the current luminescence energy range [9]. The well known advantages of FT method namely Fellgett advantage and Jacquinot (or throughput) advantage combined with a coherent excitation source [18], as we have done, can have profound influence in unraveling the fine features of luminescence processes in chalcogenide glasses.

Generally, in spectroscopy, when there is contribution to the spectra from more than one component, the spectra are deconvoluted based on the nature of the process governing each component. The luminescence process is generally described by a Gaussian line broadening mechanism in which case, the luminescence intensity can be expressed in terms of a Gaussian (amplitude version) line-shape function and can be written as [7]

$$I(h\nu) = I_0 + A\exp\left(-\frac{(h\nu - E_0)^2}{2\sigma^2}\right), \tag{2}$$

where $h\nu$ is the energy of the radiation emitted, I_0 is the offset, A is the maximum intensity or amplitude, E_0 is the energy at which the intensity is maximum and σ is the standard deviation [22]. For luminescence processes having contributions from more than one component (or transition), say n components, the expression for intensity can be written as a linear combination of contributions from individual components

$$I(h\nu) = I_0 + \sum_{i=1}^{i=n} A_i \exp\left(-\frac{(h\nu - E_{0i})^2}{2\sigma_i^2}\right) \tag{3}$$

with A_i, E_{0i} and $2.355\sigma_i$ representing, respectively, the amplitude, peak position and full width at half maximum (FWHM) of ith component or transition [22].

Based on the Gaussian line broadening mechanism discussed above for luminescence processes, the fine features in the PL spectra of different glasses were deconvoluted, as shown in Fig. 2, using the built-in Levenberg–Marquardt (LM) chi^2 minimizing algorithm available in Microcal™ Origin™ software [22,23]. The LM algorithm combines the best features of methods of linearization and gradient-descent, actively switching between the two according to the success or failure of the linear approximation. The resultant of the three deconvoluted spectra drawn along, fits well with the experimental spectra in Fig. 1. The features extracted from deconvolution exercise and area under the curve (area $= \sqrt{2\pi}A_i\sigma_i$) of respective transitions for all the three samples are listed in Table 1.

Luminescence in semiconductors occurs due to the electron–hole recombination and its origin can be traced to six different transitions as shown in Fig. 3(a) [9,24]. They are the transitions between (1) a free electron and a free hole (FE → FH), (2) an electron trapped in a shallow level and a free hole (ETSL → FH), (3) an electron trapped in a deep level and a free hole (EDTL → FH), (4) electron–hole pairs trapped in defect pairs deep in the gap (ETDL → HTDL), (5) a free electron and a hole trapped in deep level (FE → HTDL) and (6) a free electron and a hole trapped in shallow level (FE → HTSL).

Coming to the present results, all the tree transitions for each sample occur at energies far

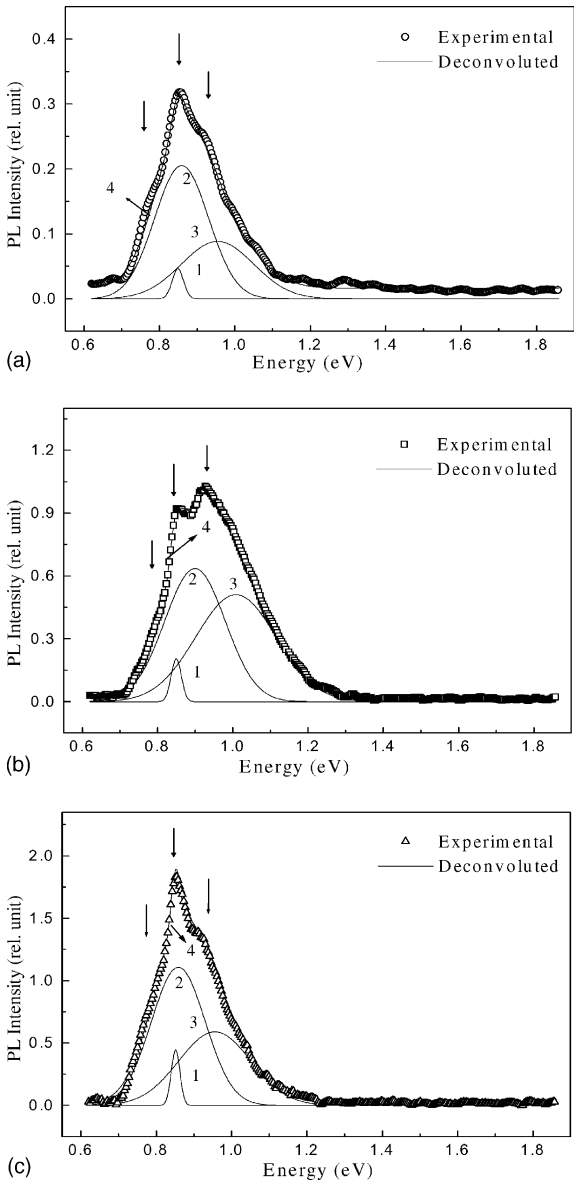

Fig. 2. Deconvoluted experimental PL spectra for (a) a-Se, (b) $Ge_{20}Se_{80}$ and (c) $Ge_{20}Se_{70}Te_{10}$ glasses. The experimental spectra are represented by symbols and the deconvoluted spectra are represented by curves 1, 2 and 3. The resultant of the three deconvoluted spectra is represented by curve 4.

less than the known band gap of these materials (~2 eV) and are largely Stokes shifted. Such a large shift of half the band gap magnitude is not feasible for a band-to-band luminescence

Table 1
The features extracted from the experimental spectra for different compositions

Sample	xc_1 (eV)	FWHM (eV)	Area, A_{a1}	xc_2 (eV)	FWHM (eV)	Area, A_{a2}	xc_3 (eV)	FWHM (eV)	Area, A_{a3}
a-Se	0.848 ± 0.003	0.034 ± 0.011	0.017 ± 0.007	0.854 ± 0.012	0.168 ± 0.020	0.372 ± 0.071	0.954 ± 0.014	0.238 ± 0.038	0.236 ± 0.040
$Ge_{20}Se_{80}$	0.849 ± 0.004	0.035 ± 0.009	0.088 ± 0.025	0.898 ± 0.008	0.188 ± 0.011	1.214 ± 0.242	1.003 ± 0.014	0.252 ± 0.019	1.021 ± 0.138
$Ge_{20}Se_{70}Te_{10}$	0.852 ± 0.001	0.030 ± 0.005	0.111 ± 0.020	0.852 ± 0.002	0.169 ± 0.007	1.867 ± 0.191	0.949 ± 0.009	0.214 ± 0.024	1.478 ± 0.118

The uncertainties in the extracted features are calculated for 95% confidence interval.

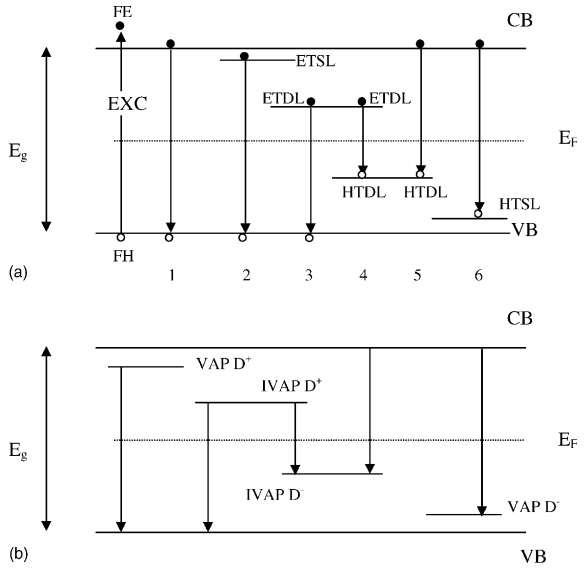

Fig. 3. (a) Six different PL transitions possible in a semiconductor involving gap states and (b) energy level scheme for gap states in chalcogenides and the transitions involving them. Further explanation can be seen in the text.

transition that occurs when free electrons recombine radiatively with free holes across the band gap [2,9]. Hence, we are left with five possible recombinations involving gap levels to identify the three deconvoluted spectra for each sample. In principle, either VAPs (random D^+ and D^-) or IVAPs (non-random D^+ and D^-) can contribute to luminescence in chalcogenide glasses [5]. The location of gap states associated with random D^+ and D^- defects as proposed by the CDB model is sketched in Fig. 3(b). According to the model, the random D^- (VAP C_1^-) center forms a shallow level close to the valence band from where it can capture a hole. Similarly, the random D^+ (VAP C_3^+) center forms a shallow level close to the conduction band from where it can capture an electron. On the contrary, in the case of non-random D^+ and D^- (or IVAPs), there exists a greater lattice distortion which can significantly modify their energies. Consequently, we expect them to lie deep in the gap in accordance with the experimental evidences for negative-U (negative correlation energy) [20]. Considering these facts, the individual deconvoluted spectra can be identified with the transitions involving these levels as discussed below.

Interestingly, as can be seen in Table 1, the peak position of one of the three deconvoluted spectra (curve 1 in Fig. 2) is at 0.85 eV for all the three samples and appears insensitive to composition. In chalcogenide glasses, the sensitivity of IVAPs to the addition of dopants is far less compared to that of VAPs [5]. On this account, we identify the insensitive deconvoluted spectra with the radiative transitions involving IVAPs (or non-random D^+ and D^-) i.e. with the transition ETDL $\rightarrow$ HTDL. With this identification, the remaining two deep level associated transitions namely FE $\rightarrow$ HTDL and ETDL $\rightarrow$ FH can be considered either less probable or improbable as it is natural for electron–hole pairs trapped at structurally close IVAP centers to recombine among themselves. To identify the two broader deconvoluted spectra (curve 2 and 3), we are then left with exactly same number of choices namely ETSL $\rightarrow$ FH and FE $\rightarrow$ HTSL. According to the CDB model, the lattice distortion at random D^+ center is relatively higher than that at D^- center and accordingly the transition involving D^+ center occurs at lesser energy than that involving D^- center. The second and third deconvoluted spectra are hence identified with ETSL $\rightarrow$ FH and FE $\rightarrow$ HTSL transitions, respectively.

Though the energy level scheme shown in Fig. 3(b) displays the possibility of more than one optical transition, it does not account for Stokes shifts of multiple transitions. This is because the energy difference between a shallow trap level for electron (hole) and valence (conduction) band edge is closer to the band gap value, but the radiative recombination transitions involving the level occurs at significantly lower energies. An appropriate way to represent such luminescence processes is the configurational coordinate diagram representation shown in Fig. 4(a) where E is plotted versus R with parabolic shape [12,24]. The difference in the equilibrium distances in the ground and excited state parabolas occurs mainly because the chemical bond length in the excited state is different from that in the ground state. Accordingly, the parabolas are shifted relative to each other over a value ΔR. The most probable optical absorption occurs at $R = 0$ of ground state and brings the center to a high vibrational level of

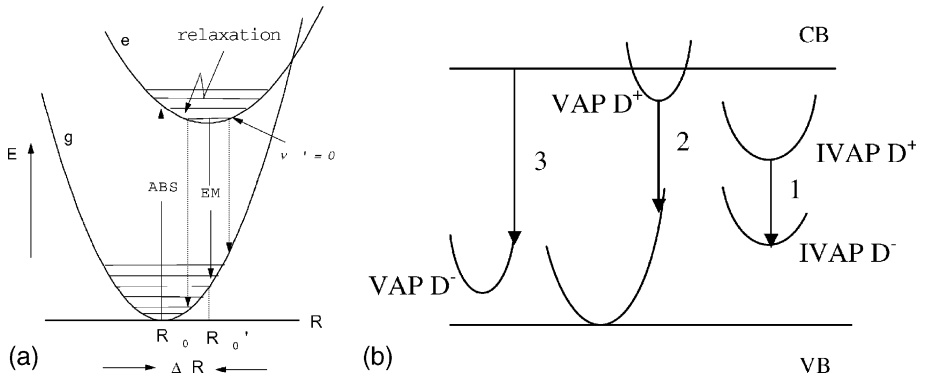

Fig. 4. (a) Configurational coordinate diagram representation of absorption and emission transitions, (b) the configurational coordinate diagram representation of multiple transitions in a chalcogenide glass semiconductor.

the excited state. The center then relaxes to the lowest vibrational level of the excited state from where it can spontaneously return to the ground state under emission of radiation. The emission occurs at a lower energy than the absorption energy due to the relaxation processes. The energy difference between the maximum of the lowest excitation band and that of the emission band is the Stokes shift. Along these lines, multiple transitions identified above can be better represented with a configurational coordinate diagram illustrated in Fig. 4(b). In this illustration, we conjecture separate configurations even for non-random D^+–D^- (IVAPs) as we believe that the energy of D^+ and D^- defects can not be the same be it a random arrangement or a non-random one. Accordingly, the radiative recombination transition at IVAPs is depicted by a transition between two deep level parallel parabolas in Fig. 4(b). Consideration of parallel parabolas is done to elucidate the smaller width of this transition compared to that of the other two as it is known that the zero-phonon optical transition between parallel parabolas is the narrowest one [24]. Other two transitions involving random D^+ and D^- defects are also represented in the same illustration to qualitatively elucidate the observed Stokes shifts.

Lastly, from Table 1, it can be seen that with the addition of Ge to Se, both the broader peaks shift to higher energy side by nearly 0.049 ± 0.028 eV. In a reverse trend, addition of Te brings back the broader transitions to their original positions as in a-Se. As it is known quite well that Ge addition introduces $GeSe_{4/2}$ structural units [25], one can expect a change in the local environment and therefore the energy of the random defect centers or VAPs. From the reversal trends in the transitions involving random defect centers it can be inferred that: (i) the presence of a lower atomic radii element Ge near random D^+ and D^- defects push the associated shallow donor and acceptor levels towards the band edge. Consequently, the associated transitions shift towards the higher energy side, (ii) presence of Te, a higher atomic radii element, can push the shallow donor and acceptor levels towards the mid-gap [24]. The resulting transitions therefore will then shift towards lower energy side. Recent PL studies in $Ge(Se_xS_{1-x})_2$ glasses show that the luminescence transition energy shifts to higher energy side with the increasing presence of S, a lower atomic radii element [26]. The study thereby substantiates the inferences drawn above.

Interestingly, recent studies on Er-doped Ge-chalcogenide glasses have shown more or less similar PL line-shapes with three radiative transitions at around the same energy range as in present investigations [27,28]. In addition, PL studies carried out by us on Bi-doped Ge chalcogenide glasses have given further insights into the influence of composition on VAP and IVAP centers [21].

5. Conclusions

In conclusion, the fine features in the PL spectra of a-Se were examined using FT spectroscopy. Similar features observed for $Ge_{20}Se_{80}$ and $Ge_{20}Se_{70}Te_{10}$ glasses are in line with the earlier results. The detailed deconvolution procedure applied for the first time to extract better information about the observed features provide signatures of radiative recombination at discrete gap levels arising due to both VAPs and IVAPs. A better description for mechanism of Stokes shifted multiple luminescence transitions in chalcogenide glasses is illustrated using a configurational coordinate diagram. The FT method utilized in the present investigations has played a significant role in capturing luminescence transitions occurring simultaneously at various defects with different lifetimes.

Acknowledgements

We thank DST and CSIR, Government of India for financial support. Thank Professor E.S.R. Gopal for informative discussions.

References

[1] K. Shimakawa, A.V. Kolobov, S.R. Elliot, Adv. Phys. 44 (1995) 475.
[2] S.R. Elliot, Physics of Amorphous Materials, Longman, London, 1990.
[3] R.A. Street, N.F. Mott, Phys. Rev. Lett. 35 (1975) 1293.
[4] M. Kastner, D. Adler, H. Fritzche, Phys. Rev. Lett. 37 (1975) 1504.
[5] E.A. Davis, in: M.H. Brodsky (Ed.), Topics in Applied Physics: Physics of Amorphous Semiconductors, Springer, Berlin, 1979, p. 41, and references therein.
[6] D.K. Schroder, Semiconductor Material and Device Characterization, John Wiley, New York, 1990, p. 490.
[7] R.A. Street, Adv. Phys. 25 (1976) 397, and reference therein.
[8] E. Mytilineou, Z. Lin, P.C. Taylor, Solid State Commun. 84 (1992) 617.
[9] S. Perkowitz, Optical Characterization of Semiconductors: Infrared, Raman and Photoluminescence Spectroscopy, Academic Press, London, 1993, p. 45.
[10] R.A. Street, D.K. Biegelsen, J. Non-Cryst. Solids 32 (1979) 339.
[11] S.G. Bishop, U. Strom, E.J. Friebele, P.C. Taylor, J. Non-Cryst. Solids 32 (1979) 359.
[12] B.A. Weinstein, Philos. Mag. B 50 (1984) 709.
[13] S.G. Bishop, D.A. Turnbull, B.G. Aitken, J. Non-Cryst. Solids 266–269 (2000) 876.
[14] K. Tanaka, J. Non-Cryst. Solids 266–269 (2000) 889.
[15] Y. Wang, T. Komamine, T. Nakaoka, O. Matsuda, K. Inoue, K. Murase, J. Non-Cryst. Solids 266–269 (2000) 904.
[16] G. Suma, H.L. Bhat, B. Sundersheshu, R.K. Bagai, V. Kumar, Appl. Phys. Lett. 68 (1996) 2424.
[17] V.P. Izvekov, M. Koos, I. KosaSomogyi, J. Non-Cryst. Solids 59&60 (1983) 1011.
[18] N.F. Mott, E.A. Davis, Electronic Processes in Non-Crystalline Solids, Clarendon, Oxford, 1979.
[19] R.A. Street, T.M. Searle, I.G. Austin, in: Proc. 12th Int. Conf. on Amorphous and Liquid Semiconductors, M.H. Pilkuhn (Ed.), Teubner, Stuttgart, p. 1037.
[20] A.V. Kolobov, M. Kondo, H. Oyanagi, A. Matsuda, K. Tanaka, Phys. Rev. B 58 (1998) 12004.
[21] N. Asha Bhat, K.S. Sangunni, K.S.R.K. Rao, J. Optoelectronics Adv. Mater. 3 (2001) 735.
[22] P.R. Bevington, Data Reduction and Error Analysis for the Physical Sciences, McGraw-Hill, New York, 1969.
[23] Available from <http://www.galactic.com/Algorithms/cf_levenberg.htm>.
[24] G. Blasse, B.C. Grabmaier, Luminescent Materials, Springer, 1994.
[25] P. Tronc, M. Bensoussan, A. Brenac, C. Sebenne, Phys. Rev. B 8 (1973) 5947.
[26] Y. Wada, Y. Wang, O. Matsuda, K. Inoue, K. Murase, J. Non-Cryst. Solids 198–200 (1996) 732.
[27] D.A. Turnbull, S.G. Bishop, J. Non-Cryst. Solids 213&214 (1997) 288.
[28] S. Ramachandran, S.G. Bishop, Appl. Phys. Lett. 73 (1998) 3196.